Synthesis and Characterization of Polyamide-66/Calcium Carbonate Composites

Aboutaleb Ghadami Jadval Ghadam[*1] and Hajir Karimi [2]
[1]Departments of Petroleum and Chemical Engineering, Yasouj Branch, Islamic Azad University, Yasouj, Iran
[2]Department of Chemical Engineering, Yasouj University, Yasouj, Iran
(Received 24 June 2014, Accepted 14 January 2015)

Abstract

Polyamide-66(PA66)/$CaCO_3$ micro- and nano-composites were prepared using a polymer solution method at filler loading of 0, 1, 2 and 3 weight percent. Nano-size of $CaCO_3$ was synthesized by micro-emulsion technique. The material was characterized by XRD, SEM, FTIR and UV-VIS techniques. XRD results of composites suggested that $CaCO_3$ particles are found in the amorphous phase of the semi-crystalline thermoplastic and α-crystalline form of thermoplastic is thermodynamically more stable than the γ-crystalline forms at room temperature. The uniform dispersion of 1, 2, and 3 wt. % surface modified micro- and nano-$CaCO_3$within PA66 were evidenced from SEM images. FT-IR analysis confirmed the chemical structure of the PA66. Absorption peaks for all required chemical groups were showed in the FTIR spectra: N-H stretch at 3305.52 cm^{-1}, C-H stretch at 2865.02-2936.45 cm^{-1}, Amide-I at 1638.76 cm^{-1}, and Amide-II at 1539.55 cm^{-1}. UV-VIS data showed that the presence of $CaCO_3$ particles in PA66 results in the decrease of energy-band gaps of the composites. In addition, the results showed that incorporation of $CaCO_3$ particles increased the modulus and tensile strength of neat PA66 however decreased its yield and elongation at break.

Keywords: Polyamide- 66, $CaCO_3$ Nanoparticle, Morphology, Optical properties, Mechanical properties, Nanocomposite

Introduction

In the last decade, organic & inorganic nanocomposites have received considerable interest in research and industrial development not only because of their intriguing properties but also for their wide range of applications [1]. Nylon-66 is a semi-crystalline material that has a combination of strength, flexibility, toughness, and abrasion resistance. It is also known for its dye-ability, low coefficient of friction (self-lubricating), low creep, and resistance to solvents, oils, bases, fungi, and body fluids.

The applications of nylon-66 range from textile fibers, membranes, tapes, food packaging to electronics and automotive parts [2]. Among the various fillers, calcium carbonate ($CaCO_3$) has been the most widely used owing to its easy availability at low cost and therefore, has been utilized as important reinforcing filler in thermoplastic industry [3]. The mechanical behavior of the polymer is also likely to be modified via the interfacial properties between the filler and the matrix. The role of interfacial adhesion between filler and matrix on the resulting mechanical properties of composites based on nylon-66 has been investigated by Sonawane and co-workers in 2010 [4]. They have reported that nano-$CaCO_3$ filled in polyamide shows the improvement in Young's modulus in comparison to commercial $CaCO_3$ as well as virgin polyamide. It was also demonstrated that with increment in weight percentage of filler loading, elongation at break decreases [4].

In this study, the microparticles (procured in the lab) and nanoparticles of $CaCO_3$ (synthesized using micro-emulsion method) were used as filler to prepare nylon-66/$CaCO_3$ micro and nanocomposite through polymer solution method. The characteristics and properties of the two composites (micro and nano) have been compared. The structural and morphological properties of composites were characterized by XRD. The optical properties of the sample were investigated by FTIR and UV-

* Corresponding author: Tel: +98 917 145 8176 Email:aghadami80@gmail.com

VIS spectrophotometers. Universal Testing Machine (UTM) was also used to measure mechanical properties (tensile tests) of composites at room temperature according to ASTM-D882.

2. Experimental

2.1. Materials

$CaCO_3$ nanoparticles with an average size of 33 nm were synthesized via micro-emulsion route [5]. $CaCO_3$ particles with an average size of 2 μm and Dimethyl Sulfoxide (DMSO), 99%, were procured from Merck Company, Germany. Injection molding grade PA66 (Nylon) polymer from SRF Limited, India was used to produce the micro and nanocomposites.

2.2. Synthesis of Micro and NanoComposites

Polymer solution method was used for the synthesis of micro and nanocomposites. Effect of the quantity of micro and nanoparticles of $CaCO_3$ on the synthesized composites was studied for 0, 1, 2 and 3 wt.%.

For preparation of polyamide-66/$CaCO_3$ composites, Polyamide-66 (PA66), micro- and nano- calcium carbonate particles were first heated in a vacuum oven for 12 hrs at 100^{o}C until any possible residual moisture was removed. Then, polyamide-66 was dissolved in DMSO until a homogeneous solution was obtained. Different amounts of $CaCO_3$ particles were carefully added to this PA66 solution under vigorous stirring with a magnetic stirrer bar at room temperature (27^{o}C). The stirring was carried out for 24 hrs under ambient condition of 27^{o}C to get the proportion of 1, 2, and 3 wt.% of nano-sized $CaCO_3$ based on PA66 content. Subsequently, the resulting solution was poured onto clean glass plates with side tapes around the glass plates (acting as thin trays) and dried until tack-free in a low-humidity chamber at room temperature. Then, the resultant films were vacuum dried for 24 hrs at 60^{o}C until all the solvent was removed by evaporation and delivered polymer nano-composite. All films were prepared for the same time and ambient conditions. Pure PA66 films were prepared in the same manner which also showed opaqueness and milk-white color upon drying of solvent. Conventional composite films were also prepared in the same procedure containing 1, 2, and 3 wt.% of micro-sized $CaCO_3$.

2.3. Characterization of the Synthesized Composites

X-ray diffraction (XRD) Analysis: the influence of micro- and nano-$CaCO_3$ particles on the crystal structure of polyamide-66 was studied using a Rigaku X-ray Powder Diffractometer with Cu anode (Cu Kα radiation, λ=1.54186 Å) in the range of $5^o \leq 2\theta \leq 30^o$ and at 30 kV and at a scanning rate of 4^o/min.

Scanning Electron Microscopy (SEM) Analysis: Scanning Electron Microscope (SEM, Carl Zeiss: EVO40) at 20 kV was used to characterize the dispersion and agglomeration of micro- and nano-$CaCO_3$ particles inside the polyamide-66 matrix. The samples were sputter-coated (Sputter Coater: POLARON-SC7640) with a thin layer (10–20 nm) of gold palladium. The coating was carried out by placing the specimen in a high vacuum evaporator and vaporizing the metal held in a heated tungsten basket. In addition, energy-dispersive x-ray spectroscopy (EDS) was also used to reveal the relative quantities of the different elements present in the compounds.

Fourier Transform Infrared Spectroscopy (FTIR) Analysis: FTIR spectroscopy is used for the identification of polymers and additives, study of coupling effects, conformational studies, crystallinity and end group analysis. FT-IR spectra were recorded with an Interspec-2020 (SPECTROLAB, UK) Spectrophotometer using KBr pellets in order to make small tablets; the analyses were conducted between 400 a 4000 cm^{-1}.

Optical Absorption Analysis: a direct and simple method for probing the band structure of composite materials is to measure the absorption spectrum. The optical absorbance A(ν) spectra for the composites were measured using a Ultraviolet-Visible (UV-VIS) Double Beam Spectrophotometer (Perkin Elmer Precisely: Lambda-35) at room temperature in the

wavelength range 200-800 nm. The absorption coefficient α(ν) was calculated from the absorbance A(ν). After correction for reflection, α(ν) was calculated using the relation (equation-1):

$$I = I_O \exp(-\alpha x) \quad (1)$$

Hence,

$$\alpha(\upsilon) = \frac{2.303}{x}\log(\frac{I_O}{I}) = \frac{2.303}{x}A(\upsilon) \quad (2)$$

Where, I_o and I are the incident and transmitted intensity, and x is the thickness of the cuvette [6]. The relationship between fundamental absorption and optical energy gap is given by equation-3:

$$E_{opt} = \frac{hc}{\lambda} \quad (3)$$

Here, c is the velocity of light. At high absorption coefficient levels for non-crystalline materials, it can be related to the energy of the incident photon by the following relation, equation-4:

$$\alpha(\upsilon) = \beta(h\upsilon - E_{opt})^n \quad (4)$$

Where, β is a constant and the exponent, n can assume values of 0.5, 1, 2, 3, and 3/2. For allowed indirect transition, the exponent takes the values 1, 2, and 3 [6].

Mechanical Properties (Tensile Tests): Tensile strength, Young's modulus and percent elongation at yield and break were measured at room temperature according to ASTM-D882 [7] by Zwick 1445 Universal Testing Machine (UTM). The test specimen (film) dimension was 7×0.8×0.09 cm^3 (*Length* ×*Width* ×*Thickness*). For each composite type, seven specimens were used and the average value of three replicated tests was taken for each composition. Subsequently, the mean values and their standard deviations were calculated. The test specimen gauge length was 5.1 cm and crosshead speed for the film testing was

0.10 cm/min.

3. Results and Discussion

3.1. XRD Analysis

Polyamide-66 (PA66) is a polycrystalline polymer in which triclinic α-crystalline and pseudo-hexagonal γ-crystalline are the most important phases. The triclinic α-phase structure at room temperature transforms into γ-phase structure at elevated temperatures. Liu, et al. (2007) have reported that even though, the stable crystalline form of PA66 at room temperature is in the α-crystalline, γ-crystalline forms can also co-exist along with the α-crystalline form depending on processing conditions [8]. XRD measurements were used to investigate the influence of $CaCO_3$ particles on the crystal structure of polyamide-66. The XRD patterns of PA66 and PA66/$CaCO_3$ micro- and nano-composites are shown in Figure 1.

It is well documented that the crystalline structure of a semi-crystalline thermoplastic has significant effect on the thermal and mechanical properties. Furthermore, XRD results of composites have suggested that $CaCO_3$ particles are found in the amorphous phase of the semi-crystalline thermoplastic. It has been found that the α-crystalline form is thermodynamically more stable and has a higher modulus than the γ-crystalline forms at room temperature [8]. As shown in Figure 1, the XRD pattern of neat PA66 (PA66 with 0 wt. % $CaCO_3$) displays two strong diffraction peaks at 2θ=19.232 and 23.280^o corresponding to the (100) and (010) (110) doublet of the α-crystalline structure. Furthermore, a small peak at 12.634^o is associated with the (002) plane of the γ-crystalline structure. It can be seen from Figure 1 that with increasing the content of $CaCO_3$ particles within polyamide-66 matrix, the γ crystalline form tends to disappear. Thus, it may be said that calcium carbonate particles form a PA66 crystal thermodynamically more stable with the reduction of the meta-stable γ crystalline phase within the polymeric matrix and forming only an α crystalline structure.

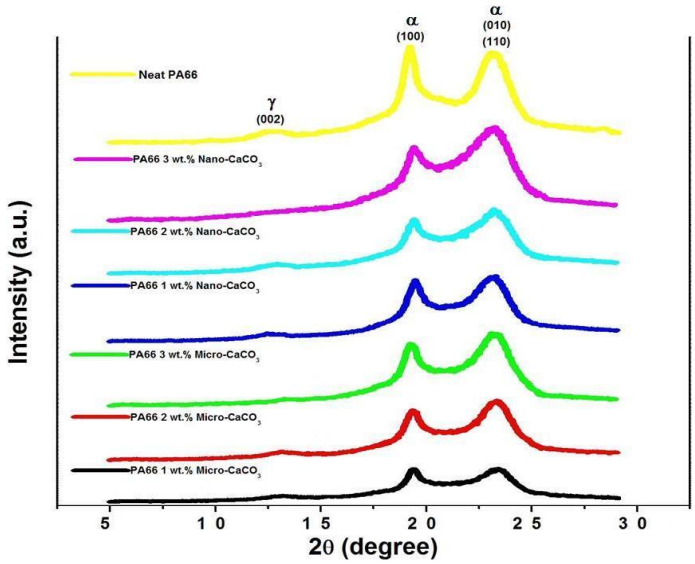

Figure 1: XRD patterns of neat PA66 and PA66/micro- and nano $CaCO_3$ composites: 1, 2 and 3 wt. % $CaCO_3$ micro- and nano-particles

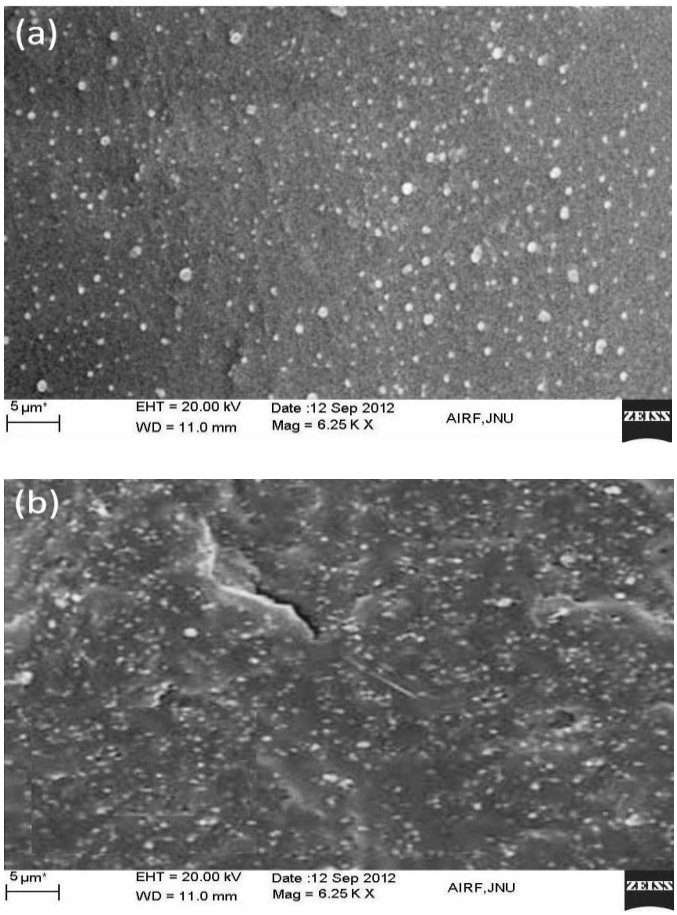

Figure 2: SEM images of PA66/CaCO3: a) Micro-composites, b) Nano-composites: magnification of 6.25 kx

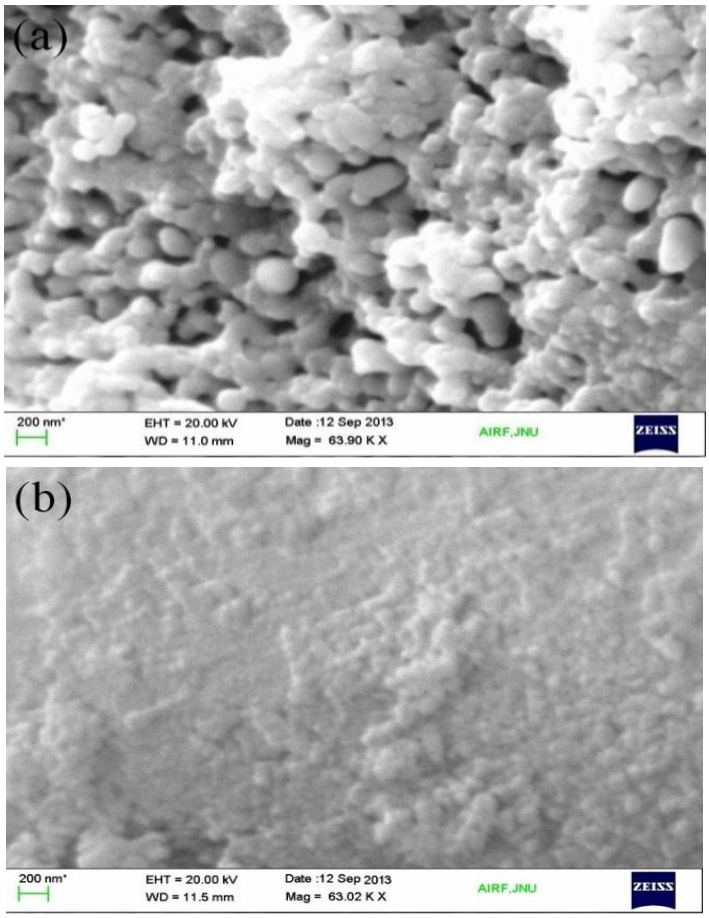

Figure 3: SEM images of PA66/CaCO3: a) Micro-composites, b) Nano-composites: magnification of 63.02 kx

3.2. SEM Analysis

The dispersion of the particles inside the bulk PA66 was investigated using SEM. It is known that the dispersion of filler in the polymer matrix can have a significant effect on the mechanical properties of the composites. However, the dispersion of inorganic filler in a thermoplastic is not an easy process. The process becomes more intricate when nano-particles are used as filler, because they have strong tendency to agglomerate. It is reported that a good dispersion can be achieved by surface modification of the filler particles [9]. The uniform dispersion of surface modified micro- and nano-$CaCO_3$ [5] within PA66 is evidenced from SEM images as shown in Figures 2 & 3. These figures show the different situation of the uniform dispersion of the calcium carbonate micro- and nano-particles in the nylon-66 through various resolutions.

It is clearly noticed from these figures that both types of surface modified, micro- and nano-particles are covered and quite welded to the PA66 matrix. Moreover, nano-fillers appear homogeneously dispersed into polymer. Referring to Figure 3(a), it can be seen that some of the cavities, in the nylon-66, are occupied by micro-$CaCO_3$ particles. However, since no cavity is observed on the surface of PA66/nano-$CaCO_3$ composites, as noticed in Figure 3(b), the presence of nano-particles must be more responsible than micro-particles for the cavitations. In the nano-composites containing coated $CaCO_3$, the particles are found better welded to the PA66 matrix. In addition, no fracture lines and cavities are present at the interface, suggesting that the

coating of $CaCO_3$ [5] promotes adhesion between the particles and PA66 matrix thus improving the compatibility between the phases. Figure 4 also shows the presence of $CaCO_3$ particles in the polymer composites.

3.3. Fourier Transform Infrared spectroscopy (FTIR) Analysis

FTIR can be used to detect amorphous or crystalline $CaCO_3$ on PA66 surfaces. FTIR spectra taken for neat PA66, PA66/$CaCO_3$ micro- and nano-composites are shown in Figure 5. The band assignments for PA66 are well documented in the literature [10]. Fourier-transform IR confirmed the chemical structure of the PA66, showing absorptions for all required chemical groups: N-H stretch at 3305.52 cm^{-1}, C-H stretch at 2865.02-2936.45 cm^{-1}, Amide-I at 1638.76 cm^{-1}, and Amide-II at 1539.55 cm^{-1}. The band at N-H stretching and C=O stretching strongly depend on hydrogen bonding interaction between the PA66 chains, these results are supported by other literature [11]. $CaCO_3$ forms a complex with C-H groups in polyamides and break the hydrogen bonds between PA66 chains, as can be inferred from Figure 5.

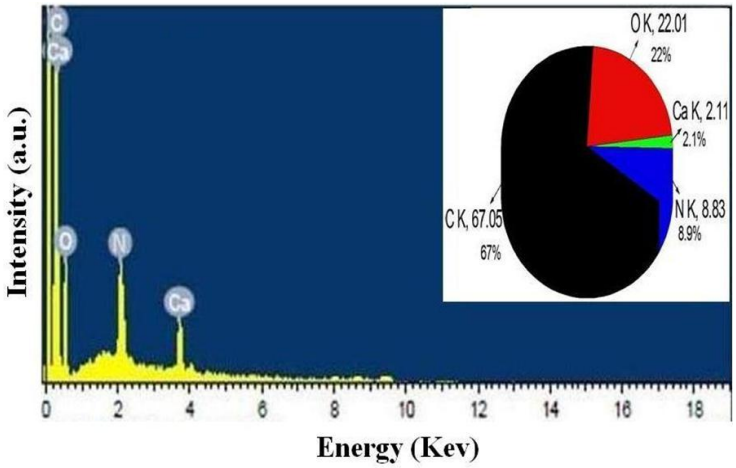

Figure 4: Energy-dispersive x-ray (EDS) spectra of PA66/CaCO3 composites

Table 1: FT-IR spectra and assignment of PA66

Wavenumbers (cm^{-1})	Assignment
3305.52	N-H stretching
3080.11	C-H asymmetric stretching
3071.38	C-H symmetric stretching
2936.45	CH_2 asymmetric stretching
2865.02	CH_2 symmetric stretching
1745.03	C=O stretching
1638.76	Amide I band
1539.55	Amide II band/CH_2 asymmetric deformation
1468.11	N-H deformation/CH_2 scissoring
1368.90	Amide III band/CH_2 wagging
1149.29	CCH symmetric bending/CH_2 twisting
1128.20	CCH symmetric bending
936.34	C-C stretching
690.29	N-H wagging/CH_2 rocking
606.23	C-C bending
579.17	O=C-N bending

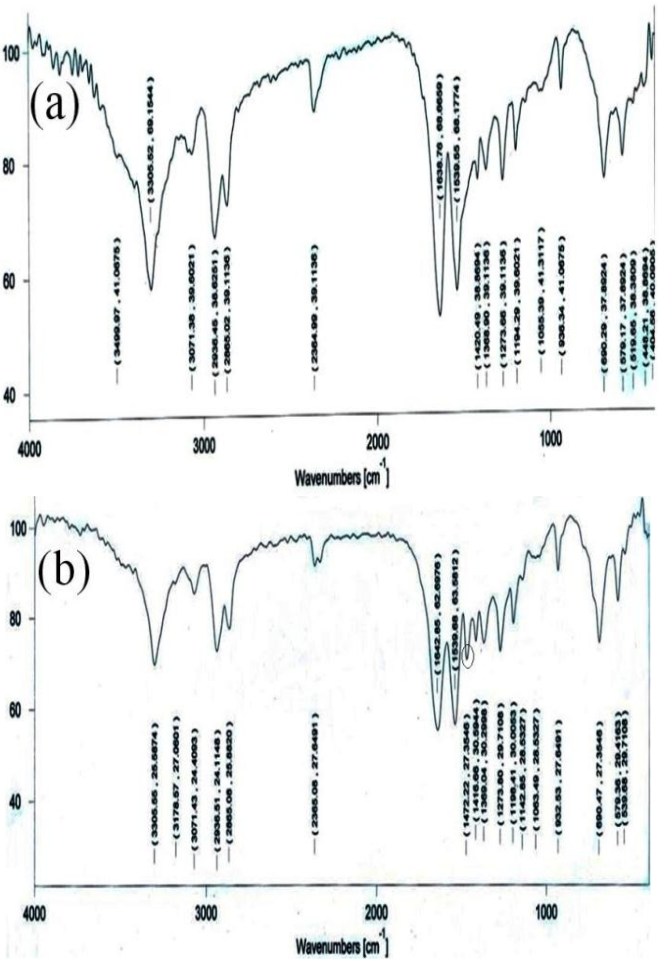

Figure 5: FT-IR spectrum of a) neat nylon-66 & b) PA66/CaCO3 composites

Therefore it is expected to see a shift in the vibration bands associated with C-H stretching vibration. The fundamental bands and probable assignments for neat PA66 and PA66/$CaCO_3$ composites are given in Tables 1 and 2. Structural changes were observed in the FTIR spectra after the addition of filler in PA66. There were some significant changes observed in the IR absorption of the C-H region at 1472.22 cm^{-1} (Strongest peak relating to $CaCO_3$ particles) between the filled and unfilled PA66.

Changes in the peaks proved that the presence of filler in the matrix affects the transmittance of the polymer. It means that the interfacial effect would be a dominant factor where there is direct binding of the polymer and the filler. These results are in good agreement with reported results by Basilia, et al. (2007) [12]. The exposed thick PA66 sample has an absorbance peak at 877 cm^{-1}.This peak is due to the absorbance of the CO_3 group and indicates the presence of $CaCO_3$; this point is supported by Suel, et al. (2004) [13]. If N-H bonds shift to higher frequency, the red shift will be caused by these bonds but in the reverse case the blue shift is caused by them due to the reduction in bond order. The primary motivation for determining the molecular structure of a polymer using FTIR spectroscopy is to relate the structures to the performance properties of the polymer in end use. If the polymer chains are completely characterized and the structural basis of its properties are known, the polymerization reaction can be optimized and controlled to produce the optimum properties from the particular chemical system [14].

Table 2: FT-IR spectra and assignment of PA66/CaCo3 composites

Wavenumbers (cm^{-1})	Assignment
3305.55	N-H stretching
3178.57	C-H asymmetric stretching
3091.43	C-H symmetric stretching
2936.51	CH_2 asymmetric stretching
2865.08	CH_2 symmetric stretching
1745.23	C=O stretching
1642.85	Amide I band
1539.68	Amide II band/CH_2 asymmetric deformation
1472.22	N-H deformation/CH_2 scissoring
1369.04	Amide III band/CH_2 wagging
1142.85	CCH symmetric bending/CH_2 twisting
1128.10	CCH symmetric bending
932.53	C-C stretching
690.47	N-H wagging/CH_2 rocking
606.23	C-C bending
579.36	O=C-N bending

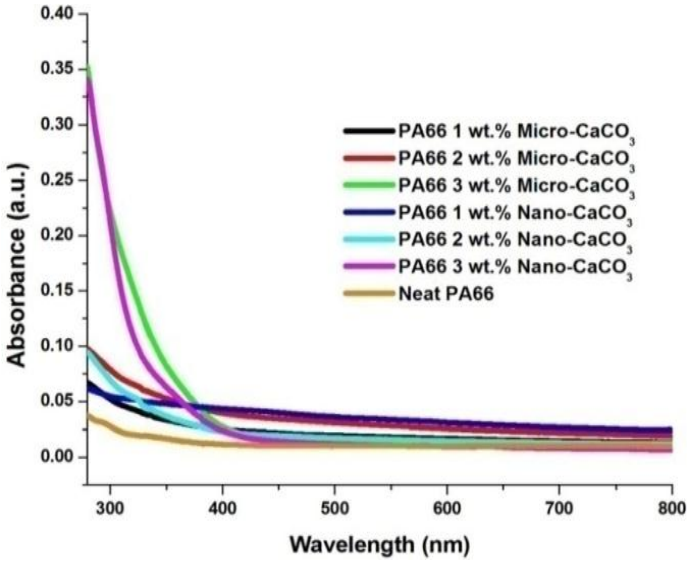

Figure 6: The optical absorption spectra for neat PA66 and PA66/$CaCO_3$ micro- and nano-composites

3.4. Optical Absorption Analysis

Optical absorption studies on neat PA66 and PA66/$CaCO_3$ micro and nanocomposites recorded at room temperature and presented in Figure 6 were carried out to obtain energy-band gaps of the samples. It may be deduced from the curves in this figure that the addition of $CaCO_3$ particles in polyamide-66 increases the UV absorbance of the composites.

In order to evaluate the energy band gaps for the composites, plots of $(\alpha h\nu)^2$ versus photon energy ($h\nu$) were obtained and showed in Figures 7-(a) - (g). The best fit to the absorption spectra in equation-4 were obtained when the value of n used was equal to 0.5, suggesting that the electron transition allowed direct transition for these nanocomposite samples.

It can be seen that the plots are linear in the region of strong absorption near the fundamental absorption edge. Thus, the absorption takes place through direct transition. The band gap obtained by extrapolating the linear part to zero of the ordinate are also indicated in the figures.

This lead to the evaluation of the band gaps, E_{opt}, while slope gives the constant value of β. The factor β depends on the transition probability and can be assumed to be constant within the optical frequency range [15]. Adding $CaCO_3$ to PA66 matrix may cause the localised states of different colour centres to overlap and extend in the mobility gap. This overlap may give an evidence for decreasing energy gap when adding $CaCO_3$ to the polymer matrix.

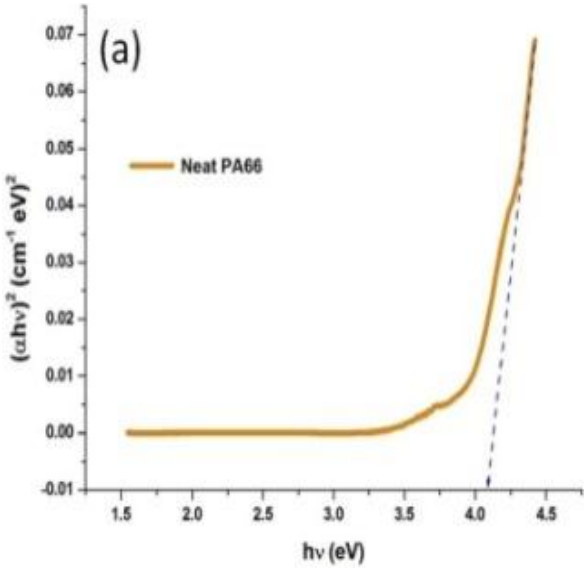

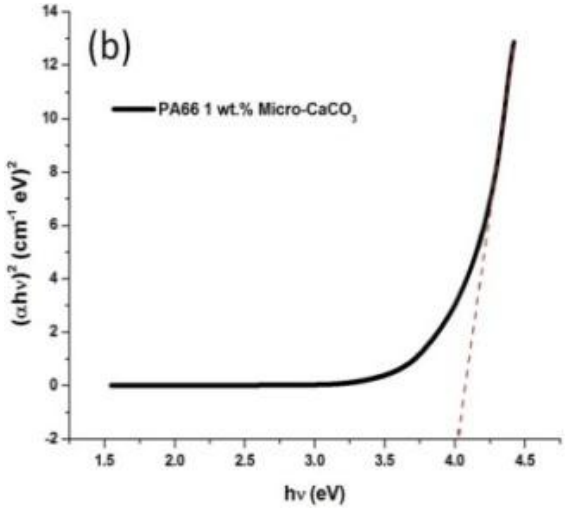

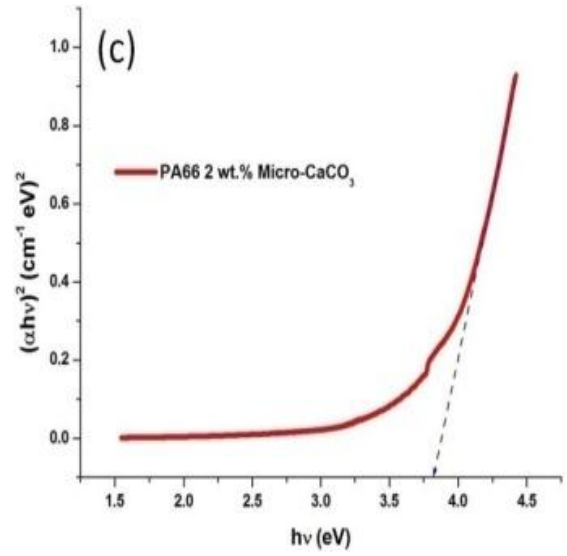
(c)
PA66 2 wt.% Micro-CaCO3
(αhν)2 (cm-1 eV)2
hν (eV)

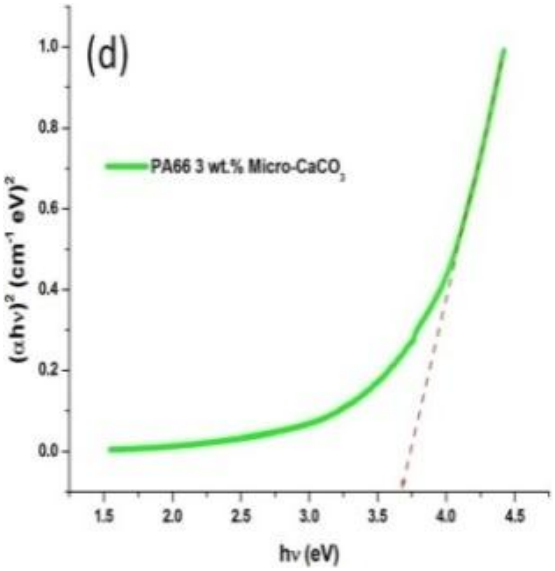
(d)
PA66 3 wt.% Micro-CaCO3
(αhν)2 (cm-1 eV)2
hν (eV)

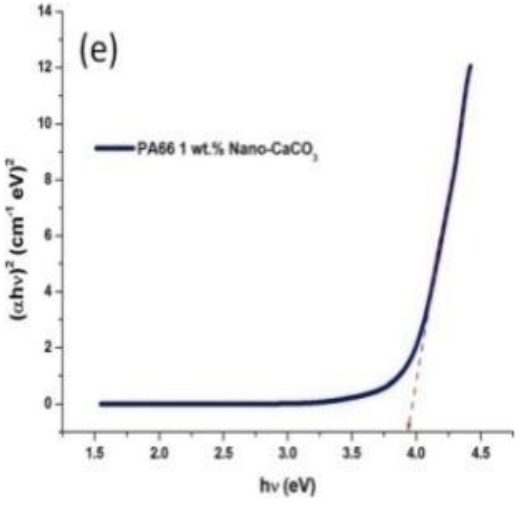
(e)
PA66 1 wt.% Nano-CaCO3
(αhν)2 (cm-1 eV)2
hν (eV)

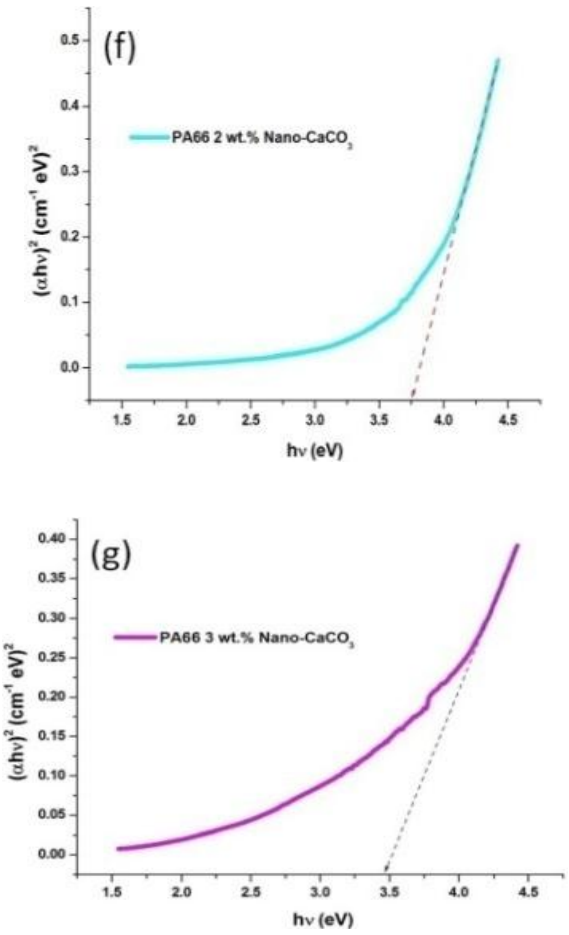

Figure 7: Evaluations of E_{opt} from optical absorption spectra of (a): neat polyamide-66 (PA66); PA66/micro-$CaCO_3$ composite (b): 1 wt. % micro-$CaCO_3$ (c): 2 wt. % micro-$CaCO_3$ (d): 3 wt.% micro-$CaCO_3$; PA66/nano-$CaCO_3$ composite (e): 1 wt. % nano-$CaCO_3$ (f): 2 wt. % nano-$CaCO_3$ (g): 3 wt. % nano-$CaCO_3$

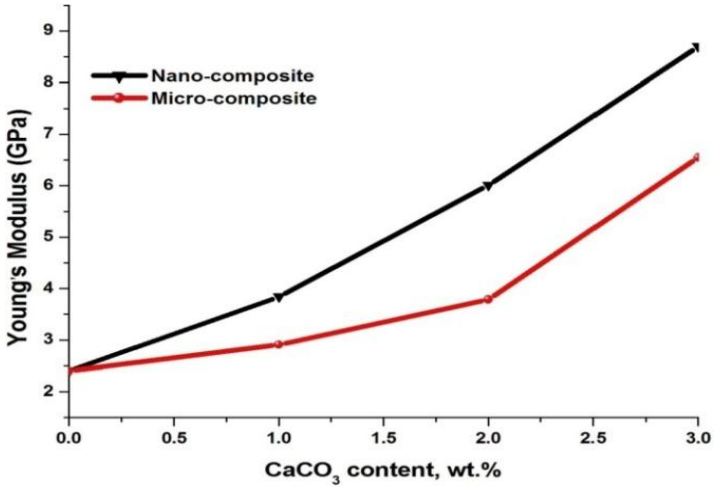

Figure 8: Effect of filler loading on the Young's modulus of micro- and nano-Polymer composites

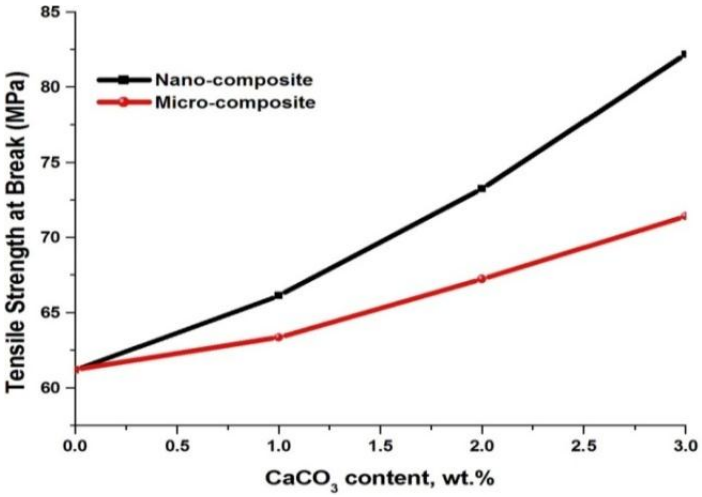

Figure 9: Variation of tensile strength of micro- and nano-composites with filler loading at break

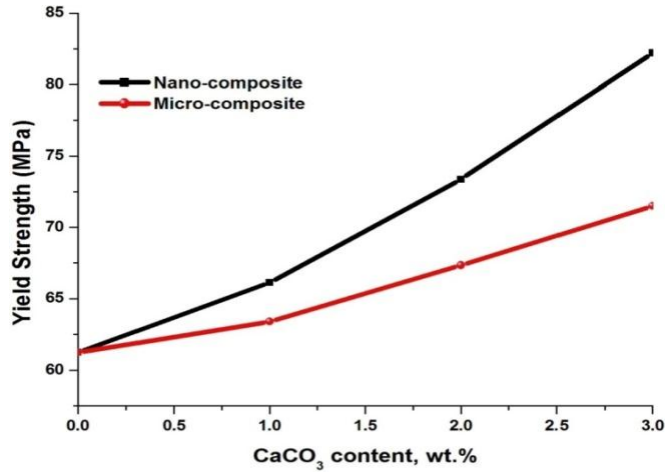

Figure 10: Variation of tensile strength of micro- and nano-composites with filler loading at yield

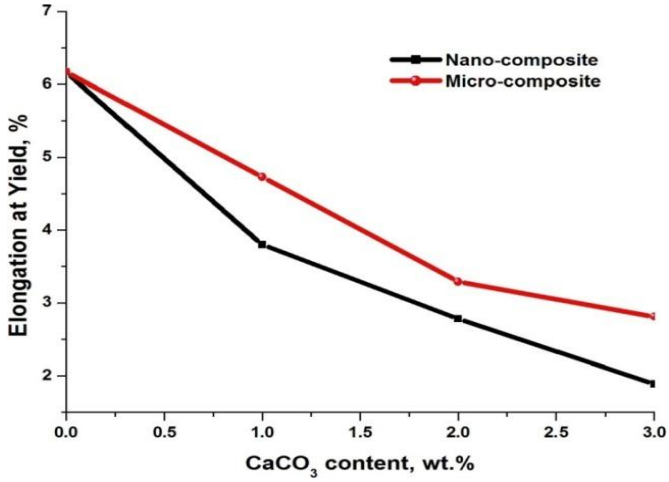

Figure 11: Variation of elongation of micro- and nano-composites with filler loading at yield

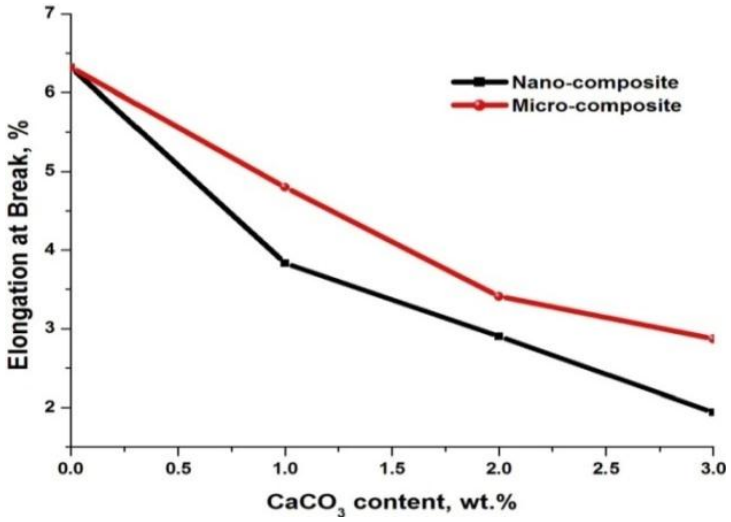

Figure 12: Variation of elongation of micro and nano-composites with filler loading at break

3.5. Tensile Properties of Composites

Tensile properties of the seven pieces of each composite sample were examined using Zwick 1445 Universal Testing Machine (UTM). For each piece of all the micro and nanocomposite samples, the stress-strain (σ-ε) data was plotted in terms of elongation. For each sample, 2-3 stress-strain (σ-ε) curves which had significant differences with the others were rejected and the tensile properties calculation was done only based on other ones. The average results were considered as the mechanical property of each sample. The calculated values of the Young's modulus of neat PA66 and PA66/$CaCO_3$ micro and nanocomposites and the effect of content of micro and nanosized $CaCO_3$ particles on the modulus of PA66/$CaCO_3$ composites are plotted in Figure 8.

It has been widely accepted that doping of the fillers into polymer matrix would improve the mechanical properties of the synthesized composites [16, 17]. The addition of the $CaCO_3$ to polymer matrix leads to improvement in stiffness for both the microcomposites and nanocomposites. The results shown in Figure 8 reveal that the Young's modulus of filled polyamide nanocomposites is higher than that of micro-$CaCO_3$-filled composites. Further, incorporation of $CaCO_3$ leads to increase in the Young's modulus of polyamide-66 composites in proportion to the filler content. This observation is attributed to the higher reinforcement effect of nano-particles compared to micro particles. Enhancement of the tensile modulus with increasing in filler content can be interpreted as follows. In general, addition of filler to polymer matrix reduces the mobility of polymer chains which causes to more stiffness or higher value of tensile modulus of the polymer composite and also this effect can be raised by increasing the amount of filler. The relationship between weight percentage of filler loading (micro- and nano-$CaCO_3$) and strength at yield and break for PA66/$CaCO_3$ micro- and nano-composites are shown in Figures 9 and 10. The tensile strength of nano-$CaCO_3$ filled polyamide composites is recorded higher than that of micro-$CaCO_3$ filled polyamide composites; the highest loading of the filler (in the range studied) shows the highest tensile strengths of composites and nano-fillers provide higher tensile strength compared to micro-$CaCO_3$. This increment in tensile strength is due to uniform dispersion of nano-filler throughout the matrix. The uniform dispersion of nano-$CaCO_3$ is confirmed by the SEM images shown in Figures 2 and 3. The reason behind higher tensile strength of nano-composites is the larger surface area of the nano-sized $CaCO_3$ particles in contact with the polymer matrix. As such, the overall bonding strength between the particles and

matrix is higher that neat samples. Thus, it is to be expected that nanocomposites could stand higher loading under external forces, as suggested by Zhu, et al., 2006 [18]. When the content of $CaCO_3$ is low, the micro- and nano-sized $CaCO_3$ cannot well disperse in the polyamide matrix and agglomerate to form a big cluster and cause a decrease in tensile strength. Elongation percent of composite samples under stress can be calculated from the relation (Equation-5), where L_o is the initial length of the test specimen, and L is the final length of sample after applying the stretching force.

$$Elongation\ Percent = \frac{L - L_o}{L_o} \times 100 \qquad (5)$$

Figures 11 and 12 show the dependence of elongation at yield and break points of composites to filler content, respectively. The incorporation of rigid fillers to polymer matrix reduces the elongation at yield and break. This is a common observation reported by earlier researchers. The results show that with increasing in weight percentage of filler loading, elongation at yield and break for micro- and nano-composites decreases. This might be due to the hard nature of polyamide as well as nano-inorganic filler and also the increment in numbers of spherulites formation with reduction in size and increase in percentage of filler. This may be attributed to the fact that $CaCO_3$ particles included into the PA66 matrix restrict the movement of polyamide chains. In other words, with the enhancement in rigidity, the ductility of composites decreases; consequently the composites break at lower elongation as explained by Zhu, et al., in 2006 [18].

4. Conclusions

PA66/$CaCO_3$ micro and nanocomposites with loading of 0, 1, 2 and 3 wt. % of the microparticles (2 μm) and nanoparticles (33 nm) were successfully prepared using polymer solution method. The XRD results of composites have suggested that $CaCO_3$ particles can form a thermodynamically stable PA66 crystal with the reduction of the meta-stable γ-crystalline phase within the polymeric matrix and forming only an α-crystalline structure. The uniform dispersion of 1, 2, and 3 wt. % surface modified micro- and nano-$CaCO_3$ within PA66 were evidenced from SEM data. The SEM results also showed that both types of the surface modified, micro and nanoparticles are covered and quite welded to the PA66 matrix. Moreover, nanofillers appear homogeneously dispersed into polymer.

FT-IR confirmed the chemical structure of the PA66 showing absorptions for all required chemical groups: N-H stretch at 3305.52 cm^{-1}, C-H stretch at 2865.02-2936.45 cm^{-1}, Amide-I at 1638.76 cm^{-1}, and Amide-II at 1539.55 cm^{-1}. Structural changes were observed in the FT-IR spectra after the addition of filler in PA66. There were some significant changes observed in the IR absorption of the C-H region at 1478.87 cm^{-1} between the filled and unfilled PA66. Changes in the peaks proved that the addition of filler in the matrix affects the transmittance of that polymer. UV-VIS data proved that addition of $CaCO_3$ particles in PA66, results in the decrease of energy-band gaps of the composites, and the values are less than that for neat PA66. In addition, the results showed that adding $CaCO_3$ micro- and nano-particles increased the modulus and tensile strength of neat PA66 but decreased its elongation at yield and break. As a result, the nano-$CaCO_3$ particles cause to more effective reinforcement of structure and therefore fabrication of a stiffer composite.

Acknowledgment

This scientific product was extracted through a research project implemented from funding of research projects of Yasouj Branch, Islamic Azad University.
In addition, active cooperation and full support of the Chairmen, Departments of Chemistry and Applied Physics, Aligarh Muslim University, Aligarh, India in providing instrumental facilities at their disposal is deeply acknowledged.

References:

1- Avella, M., Cosco, S., Lorenzo, M.L., Pace, E.D. and Errico, M.E. (2005). "Influence of $CaCO_3$ nano-particles shape on thermal and crystallization behavior of isotactic polypropyelene based nano-composites." *J. Therm. anal. Calorimet.*, Vol. 80, No. 1, pp. 131-136.

2- Jia, X., Herrera-Alonso, M. and Mc-Carthy, T.J. (2006). "surface modification; Part 1: Targeting the amide groups for selective introduction of reactive functionalities." *Polym.*, Vol. 47, No. 14, pp. 4916-4924.

3- Miao, S. (2003). "Investigation on NIR coating mechanism of PS-b-PAA coated calcium carbonate particulate." *App. Surf. Sci.*, Vol. 220, No. 1-4, pp. 298-303.

4- Sonawane, S.S., Mishra, S. and Shimpi, N.G. (2010). "Effect of Nano-$CaCO_3$ on Mechanical and Thermal Properties of Polyamide Nano-composites." *Polym. Plast. Tech. and Eng.*, Vol. 49, pp. 38-44.

5- Ghadami, J.G.A. and Idrees, M. (2013). "Characterization of $CaCO_3$ Nanoparticles Synthesized by Reverse Microemulsion Technique in Different Concentrations of Surfactants." *Iran. J. Chem. Chem. Eng.*, Vol. 32, No. 3, pp. 27-35.

6- Davis, E.A. and Mott, N. (1970). "Conduction in noncrystalline systems: V. Conductivity, optical absorption, and photoconductivity in amorphous semiconductors. " *Phil. Mag*., Vol. 22, No. 179, pp. 903-922.

7- Brendan, R. (2002). "Thin film testing - ASTM D882, in 'Annual Book of ASTM Standards." *ASTM International Publisher*, Philadelphia, Vol. 1, pp. 160.

8- Liu,Y., Cui, L., Guan, F., Gao, Y., Hedin, N.E. and Fong, H. (2007). "Crystalline morphology and polymorphic phase transitions in electrospun nylon-6 nanofibers." *Macromol.*, Vol. 40, No. 17, pp. 6283-6290.

9- Chen, M., Feng, Y., Wang, L., Zhang, L. and Zhang, J. (2006). "Study of palladium nano-particles prepared from water-in-oil micro-emulsion. " *Collo. Surf. A: Physicoch. Eng. Aspec.*, Vol. 281, No. 1-3, pp. 119–124.

10- Arimoto, H. (1964). "α–γ Transition of nylon-6." *J. Polym Sci, Part A*, Vol. 2, No. 5, pp. 2283-2295.

11- Kohan, M.I. (1973). "Nylon Plastics." John Wiley & Sons, New York.

12- Basilia, B.A., Panganiban, M.E.G., Collado, A.A.V. and De Yro, P.A. (2007). "Study on the functionality of nano-precipitated calcium carbonate as a filler in thermoplastics." *J. Sol. Mech. Mater. Eng.*, Vol. 1, No. 4, pp. 564-570.

13- Suel, S.D., Lee, S.R. and Kim, Y.H. (2004). "Poly (methyl methacrylate) Encapsulation of Calcium Carbonate Particles." *J. Poly. Sci.; Part A:Polym. Chem.*, Vol. 42, No. 16, pp. 4063-4073.

14- Charles, J., Ramkumaar, G.R., Azhagiri, S. and Gunasekaran, S. (2009). "FTIR and Thermal Studies on Nylon-66 and 30% Glass Fibre Reinforced Nylon-66." *E-J.Chem.*, Vol. 6, No. 1, pp. 23-33.

15- Zaki, M.F. (2008). "Gamma-Induced Modification on Optical Band Gap of CR-39 SSNTD." *Braz. J. Phys.*, Vol. 38, No. 4, pp. 558-562.

16- Cayer-Barrioz, J., Ferry, D., Frihi, K., Cavalier, R. and Seguela, G.V. (2006). "Microstructure and Mechanical Behavior of Polyamide 66-Precipitated Calcium Carbonate Composites: Influence of the Particle Surface Treatment." *J. Appl. Polym. Sci.*, Vol. 100, pp. 989–999.

17- Hanim, H., Zarina, R., Ahmad, M.Y.F., Mohd, Z.A. and Hassan, A. (2008). "The Effect of Calcium Carbonate Nanofiller on the Mechanical Properties and Crystallisation Behaviour of Polypropylene." *Malay. Polym. J.*, Vol. 3, No.12, pp. 38-49.

18- Zhu, B.K., Xie, S.H., Xu, Z.K. and Xu, Y.Y. (2006). "Preparation and properties of the polyimide/multi-walled carbon nano-tubes (MWNTs)." *Compos. Sci. Technol.*, Vol. 66, pp. 548-554.